

Steven A. Smith<sup>1</sup> and Ivatury S. Raju<sup>2</sup>

## EVALUATION OF STRESS-INTENSITY FACTORS USING GENERAL FINITE-ELEMENT MODELS

---

**REFERENCE:** Smith, S.A. and Raju, I.S. ,”**Evaluation of Stress-Intensity Factors Using General Finite-Element Models,**” *Fatigue and Fracture Mechanics: 29th Volume, ASTM STP 1321*, T.L. Panontin and S.D. Sheppard, Eds., American Society for Testing and Materials, 1998.

**ABSTRACT:** Finite-element methods are commonly used to evaluate the Mode I stress-intensity factor for cracked solids. Some of the methods that are used to extract stress-intensity factor values from finite-element analyses are the Crack-Opening-Displacement (COD) method, the Force method, the Virtual Crack Closure Technique (VCCT) and the Equivalent Domain Integral (EDI) method. The COD method, Force method and the VCCT appear to require that the finite-element mesh intersect the crack front in an orthogonal manner in order to obtain accurate stress-intensity factor values. The EDI does not appear to require this orthogonality with the crack front to obtain accurate stress-intensity factor values. The objectives of this study are to determine if accurate stress-intensity factor values can be obtained from finite-element models that lack orthogonality with the crack front and, if accurate values cannot be obtained, to modify the extraction methods so that accurate stress-intensity factor values can be obtained from models without orthogonality at the crack front.

Models of a through-the-thickness crack in plane strain, an embedded elliptic crack, and a semi-elliptic surface crack were created with and without orthogonality at the crack front. The models with orthogonality at the crack front were termed orthogonal models while the models without orthogonality the crack front were termed general models. Stress-intensity factors were evaluated for both the orthogonal and general models using the COD method, Force method, VCCT, and EDI method. The stress-intensity factor values obtained from these models were compared to accepted reference solutions to determine their accuracy. The COD method, Force method, and VCCT were not able to extract accurate stress-intensity factor values from general models. The EDI method was not affected by the lack of orthogonality at the crack front.

The COD method, Force method, and VCCT were modified for application to general models. These new formulations do not require the finite-element mesh to be orthogonal to the crack front. The values of the stress-intensity factors obtained from the general models using the new formulations of the extraction methods are of the same accuracy as those obtained from the models with orthogonality at the crack front.

**KEYWORDS:** finite-element method, stress-intensity factor, crack front mesh normality, finite-element modeling, three-dimensional computational fracture mechanics

---

<sup>1</sup> Graduate Research Assistant, NC A&T State University, Dept. Mech. Engr., Greensboro, NC 27411

<sup>2</sup> Head, Mechanics of Materials Branch, Materials Division, NASA Langley Research Center, MS 188E, Hampton, Virginia 23681-0001

Stress-Intensity factors are important parameters in the prediction of fracture strength, fatigue crack growth, and life for metallic components. Analytical solutions for the stress-intensity factor are difficult to obtain for complex crack configurations. Hence numerical methods are used to evaluate stress-intensity factors for three-dimensional crack problems. The finite-element method (FEM) is commonly used to analyze three-dimensional (3D) crack configurations. Stress-intensity factor values can be obtained from the results of finite-element analyses (FEA) using various post-processing methods such as the Crack-Opening Displacement (COD) method [1], the Force method [2,3], the Virtual Crack Closure technique (VCCT) [4,5], and the Equivalent Domain Integral (EDI) method [6-9].

The COD method, Force method, and VCCT are direct methods; stress-intensity factors are evaluated directly from nodal forces and displacements. The EDI is an indirect method; stress-intensity factors are evaluated using a numerical integration of stresses and strains within elements of the model. The direct methods (COD, Force, VCCT) appear to require that the finite-element mesh intersect the crack front in an orthogonal manner which will be rigorously defined in the next section. The EDI does not appear to require any mesh orthogonality with the crack front. Requiring the finite-element mesh to be orthogonal to the crack front can greatly increase the difficulty of modeling three-dimensional solids that contain cracks. Thus, understanding why some methods may require mesh orthogonality at the crack front and developing methods that do not require this condition is important.

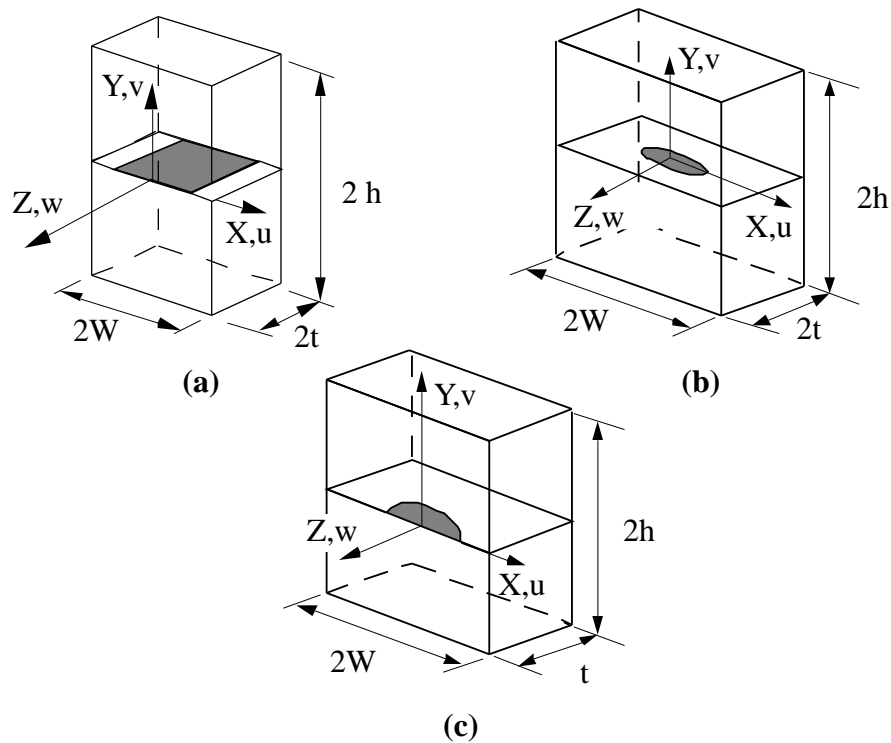


**Figure 1.** Crack configurations studied - *a) Through-the-thickness crack, b) Embedded elliptic crack, c) Semi-elliptic surface crack.*

The objectives of this study are two-fold. First, to evaluate the accuracy of the stress-intensity factor values obtained from general finite-element models (models that do not maintain orthogonality between the finite-element mesh and the crack front) using methods such as the COD method, Force method, VCCT and the EDI method. Second, to develop new formulations of the extraction methods and to evaluate the accuracy of the stress-intensity factor values obtained from general models using these new formulations.

Finite-element models, with and without orthogonality at the crack front, were created for solids with through-the-thickness cracks, embedded elliptic cracks, and semi-elliptic surface cracks (see Fig. 1). Stress-intensity factors were calculated for both the orthogonal and general models for each of these configurations using the COD method, the Force method, the VCCT, and the EDI method. The stress-intensity factor values obtained from the orthogonal and general models using these methods were compared to the reference solutions for each crack configuration. Next, formulations of the direct methods were developed specifically for application to general models. The stress-intensity factor values obtained using the new formulations were compared to the reference values for each configuration to establish their accuracy.

### **Three-Dimensional Stress-Intensity Factor Calculations**

The numerical techniques commonly used to evaluate the stress-intensity factor were first developed to analyze two-dimensional idealizations of three-dimensional crack configurations. In two-dimensional crack problems a singular point was defined as a crack tip. A crack front was assumed to extend out-of-plane away from this point, but assumptions were made so that the stresses along the crack front could be assumed to remain constant. This limited the problems that could be studied to solids with cracks that had straight or circular crack fronts. The nodes extending ahead of and behind the crack tip were forced to lie in the plane that contained the crack tip and therefore were along the normal to the assumed crack front. Hence, two-dimensional finite-element meshes were orthogonal to the crack front and the numerical methods developed to analyze the stress-intensity factor were based on this condition [1,2,4].

As more powerful computers became available and better software was developed for modeling solids, researchers began modeling three-dimensional solids with cracks. The two-dimensional methods that had been used to analyze stress-intensity factor were extended to three-dimensions. The implicit assumption that the finite-element mesh remain orthogonal to the crack front was extended as well [2,3,5-7]. It should be expected that the COD method, Force method and VCCT would not yield accurate stress-intensity factor values if used to analyze general finite-element models. The exception to this trend in formulation was the development of the EDI method which was based on the J-integral, a line integral quantity. In two-dimensions the line integral was transformed into an integration over an area, in three-dimensions, an integration over a volume [6-9]. The two- and three-dimensional formulations of the EDI made no assumptions about the finite-element mesh.

Two-dimensional crack problems are an idealization of three-dimensional problems. Three-dimensional stress-intensity factor extraction methods should not be considered extensions of two-dimensional analysis techniques. In order to obtain accurate stress-intensity factor values using the direct methods, modifications to the original formulations are required. The modifications that are necessary must take into account the lack of orthogonality between the finite-element mesh and the crack front.

#### *Orthogonality at the Crack Front*

Consider a general curved crack front configuration in the crack plane as shown in Fig. 2. This figure shows finite-element modeling of a portion of the crack front region for models with and without orthogonality at the crack front. An orthogonal mesh is shown in fig. 2(a). In a mesh with orthogonality at the crack front the nodes that are used to calculate stress-intensity factor (the nodes on the crack front, ahead of the crack front, and behind the crack front) are in the plane of the crack and lie on the normals to the crack front. In a general model, as shown in Fig. 2(b), the nodes  $p$  and  $p'$  are in the crack plane, but do not lie along the normal to the crack front. In order to obtain accurate stress-intensity factor values

the direct methods seem to require the nodes ahead of the crack front (force nodes) and the nodes behind the crack front (opening nodes) lie on the normals to the crack front.

The direct methods use the force and opening nodes to calculate a radial distance from the crack front. The radial distance is then used in an analysis with the value of the force in the y-direction and crack-opening-displacement (COD) at the force and opening nodes to determine the stress-intensity factor. When the finite-element mesh is not orthogonal with the crack front, the distance between the crack front node  $j$  and the nodes  $p$  or  $p'$  is not the value of radial distance required by the COD method, Force method, and VCCT. Furthermore, if the stresses vary along the crack front, the values of force and COD at nodes  $p$  and  $p'$  differ from the values that would be calculated at points along the normal curve. Thus, in order to obtain accurate stress-intensity factor values from general models new formulations are required.

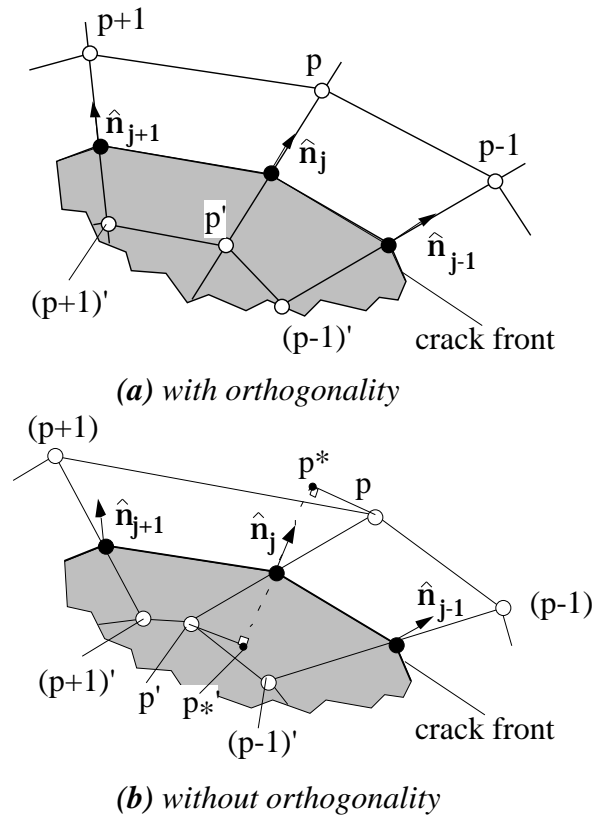
The following methodology is proposed for the evaluation of stress-intensity factor when using general models. First, the average normals of each node on the crack front must be determined as will be described the next section. Then the locations of points on the normal to the crack front ahead of and behind the crack front can be obtained from the general model by projecting the nodes of the finite-element mesh onto the average normals to the crack front. These projected points are shown as points  $p^*$  and  $p^{*}$ ' in Fig. 2(b).

The values of force or COD at the points  $p^*$  and  $p^{*}$ ' could be calculated by interpolating the values from the nodes of the model. This interpolation could be accomplished using the element shape functions. However, because the points  $p^*$  and  $p^{*}$ ' are located very near the crack front (a line singularity) the interpolated values of force and displacement at these points are not expected to be accurate. Thus, the values of force or displacement evaluated at the nodes  $p$  and  $p'$  of the finite-element mesh are preferable.

The radial distance and average element thickness or crack-extension area associated with each crack front node are determined using the projected points  $p^*$  and  $p^{*}$ ' and the crack front nodes  $j-1$ ,  $j$ , and  $j+1$ . The force at node  $p$  and the COD at node  $p'$  along with the modified values of radial distance and average element thickness or crack extension area are used in the COD method, Force method, and VCCT. The details of the evaluation of the specific quantities in this procedure are discussed below.

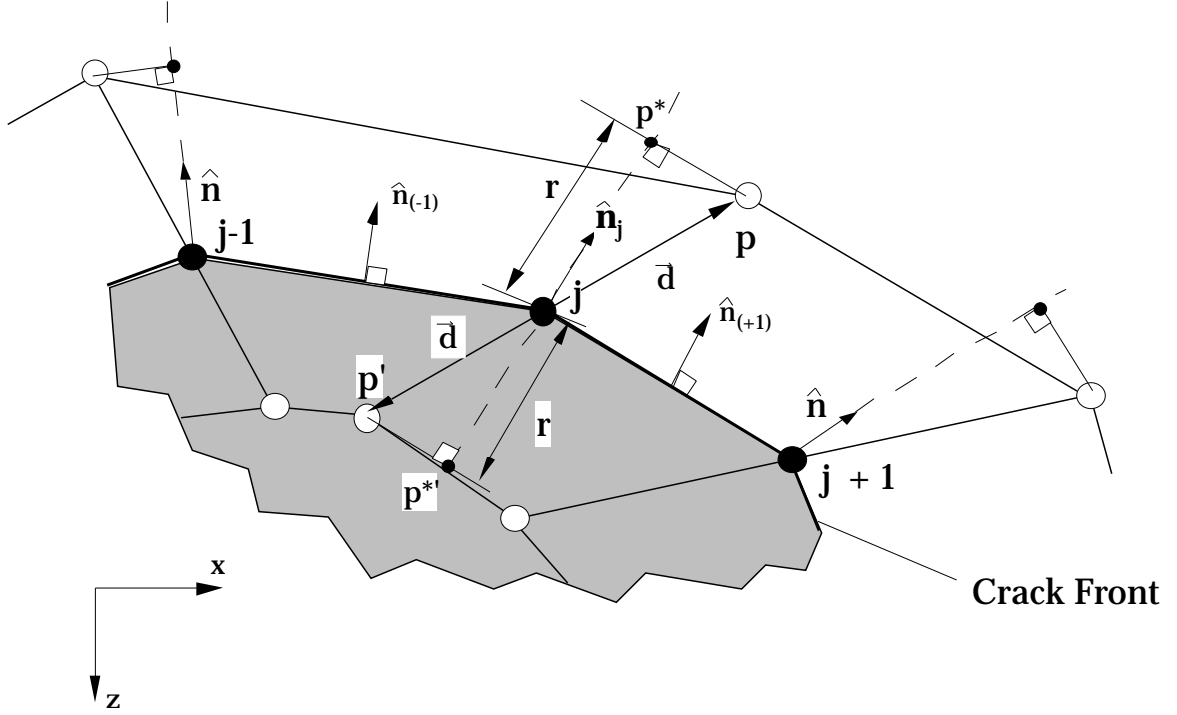
### Average Normals

Figure 3 shows nodes and element boundaries on the crack plane and near the crack front. The crack front is idealized by a piece-wise series of linear segments that are termed layers. Two layers (the  $i^{\text{th}}$  and  $(i+1)^{\text{th}}$ ) are shown in this figure. The nodes  $j-1$ ,  $j$ , and  $j+1$



**Figure 2.** Crack fronts with and without orthogonality.

are crack front nodes and the stress-intensity factor will be evaluated at node  $j$ . The nodes  $p$  and  $p'$  are the force and opening nodes, respectively, and lie on the crack plane ahead of and behind the crack front. The unit normal to the line segment connecting node  $j$  and node  $j-1$  is denoted by  $\hat{\mathbf{n}}_{(-1)}$ . The unit normal to the line segment connecting node  $j$  and node  $j+1$  is denoted by  $\hat{\mathbf{n}}_{(+1)}$ . The unit normal to the crack front at node  $j$  is shown as  $\hat{\mathbf{n}}_j$ , which is the average of the normals  $\hat{\mathbf{n}}_{(-1)}$  and  $\hat{\mathbf{n}}_{(+1)}$ .



**Figure 3.** The crack plane of a general model.

Normals to the line segments adjacent to node  $j$ ,  $\hat{\mathbf{n}}_{(-1)}$  and  $\hat{\mathbf{n}}_{(+1)}$ , can be constructed from the slope of each line segment. The slope of the normal to a line segment is given by the negative inverse of the slope of the line segment. This yields two expressions for unit vectors that are normal to the line segments adjacent to the node  $j$ . The expressions for these vectors in terms of the nodal coordinates are

$$\hat{\mathbf{n}}_{(-1)} = \frac{\frac{z_j - z_{j-1}}{x_j - x_{j-1}}}{\sqrt{\frac{z_j - z_{j-1}}{x_j - x_{j-1}}^2 + 1}} \hat{\mathbf{i}} - \frac{1}{\sqrt{\frac{z_j - z_{j-1}}{x_j - x_{j-1}}^2 + 1}} \hat{\mathbf{k}}$$

and

(1)

$$\hat{\mathbf{n}}_{(j+1)} = \frac{\frac{z_j - z_{j+1}}{x_j - x_{j+1}}}{\sqrt{\frac{z_j - z_{j+1}}{x_j - x_{j+1}}^2 + 1}} \hat{\mathbf{i}} - \frac{1}{\sqrt{\frac{z_j - z_{j+1}}{x_j - x_{j+1}}^2 + 1}} \hat{\mathbf{k}}$$

where  $\hat{\mathbf{i}}$  and  $\hat{\mathbf{k}}$  are unit vectors along the  $x$ - and  $z$ - directions, respectively, and  $x$  and  $z$  are the coordinates of the nodes ( $= j-1, j, j+1$ ) on the crack front. The average unit normal to the crack front at node  $j$  is calculated by

$$\hat{\mathbf{n}}_j = \frac{\hat{\mathbf{n}}_{(j-1)} + \hat{\mathbf{n}}_{(j+1)}}{|\hat{\mathbf{n}}_{(j-1)} + \hat{\mathbf{n}}_{(j+1)}|} \quad (2)$$

### Radial Distance

A vector  $\bar{\mathbf{d}}$  can be constructed from node  $j$  to node  $p$  or from node  $p'$  to  $j$  using

$$\bar{\mathbf{d}} = (x_p - x_j) \hat{\mathbf{i}} + (z_p - z_j) \hat{\mathbf{k}}$$

(3)

and similarly

$$\bar{\mathbf{d}} = (x_j - x_{p'}) \hat{\mathbf{i}} + (z_j - z_{p'}) \hat{\mathbf{k}}$$

This expression assumes that nodes  $p$  and  $p'$  are located equal distances from the crack front. A point on the normal to the crack front is found by projecting the vector  $\bar{\mathbf{d}}$  onto the normal  $\hat{\mathbf{n}}_j$ . This is accomplished by taking the dot product of the two vectors. This dot product is expressed in the form

$$r = \hat{\mathbf{n}}_j \cdot \bar{\mathbf{d}} = |\bar{\mathbf{d}}| \cos \theta \quad (4)$$

where  $\theta$  is the angle between the vectors  $\hat{\mathbf{n}}_j$  and  $\bar{\mathbf{d}}$ . The distance,  $r$ , and the normal vector,  $\hat{\mathbf{n}}_j$ , define the location of the points  $p^*$  and  $p^{*}$  in relation to the crack front node  $j$  (see Fig. 3).

### Average Element Thickness and Crack-Extension Area

Average element thickness and crack-extension area values are required for the Force method and VCCT, respectively (Fig. 4). These values can be calculated for a general mesh in the following manner. The average thickness for the  $i^{\text{th}}$  layer is given as

$$t_i = \frac{(t_a)_i + (t_b)_i}{2} \quad (5)$$

where  $t_a$  is the distance between the projected points that bound the  $i^{\text{th}}$  layer and  $t_b$  is the distance between crack tip nodes in the  $i^{\text{th}}$  layer. The average thickness of the  $i^{\text{th}}$  and  $(i+1)^{\text{th}}$  layer are used for determining the stress-intensity factor at the crack tip node  $j$ .

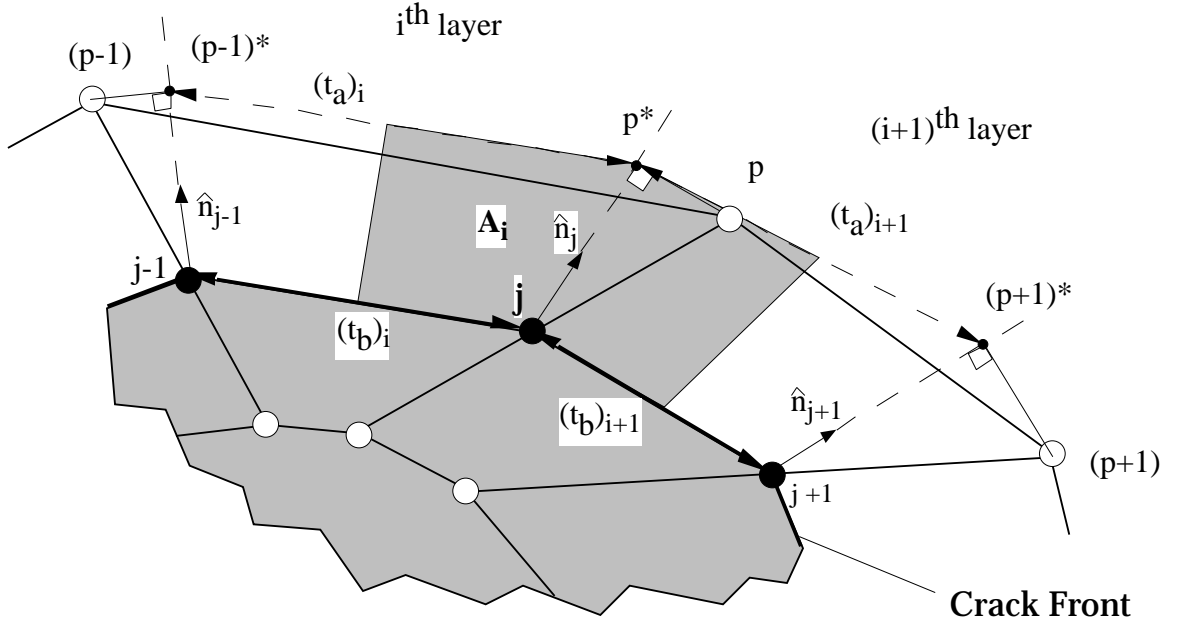


**Figure 4.** Nodes and element boundaries on the crack plane near the crack front of a general finite-element model.

The crack-extension area of the  $i^{\text{th}}$  layer is determined by multiplying the average thickness of the layer by the “height” of the layer. The “height” of the layer is calculated by taking the dot product of the vector connecting the crack tip node  $j$  and the projected point  $p^*$  and the vector normal to  $i^{\text{th}}$  segment of the crack front (see Figs. 3 and 4). This yields an expression for the area in the form

$$A_i = h_i t_i \quad (6)$$

where  $h_i$  is calculated by

$$h_i = \hat{\mathbf{n}}_{(j-1)} \cdot (\hat{\mathbf{n}}_j \cdot \bar{\mathbf{d}}) \hat{\mathbf{n}}_j \quad (7)$$

The average of the crack-extension area of the  $i^{\text{th}}$  and  $(i+1)^{\text{th}}$  layers (shown as the hatched region in Fig. 4) is used in calculating the stress-intensity factor at the crack front node  $j$ .

Slight changes to the methods of calculating average element thickness and crack-extension area are required for the first and last nodes of the crack front in models created using symmetry boundary conditions or for models that have free surfaces. Average normals are not available for these layers. Instead a normal vector is created parallel to the edge of the model. The thickness and area calculations are calculated as described above using only the quantities available from the first and last layers along the crack front.

## General Models

Two types of general models, rotated and scaled, were developed to study the effect of the lack of orthogonality at the crack front. To develop the rotated models a two-step procedure is followed. In the first step a normal model is created and a volume near and around the crack front is identified. In the second step, the nodes within the identified volume are given a rotation of  $\theta$ -degrees about the local axis normal to the crack front (see Fig. 5(a)).

The scaled model was developed to create general models for embedded elliptic and semi-elliptic surface crack configurations. First a model with a circular or part circular crack configuration is developed. Then a constant scaling factor was applied to the  $x$ -coordinates of the nodes in the model to create an elliptic model. This procedure produces a general model with an elliptic crack front modeled by piece-wise linear segments (see Fig. 5(b)).

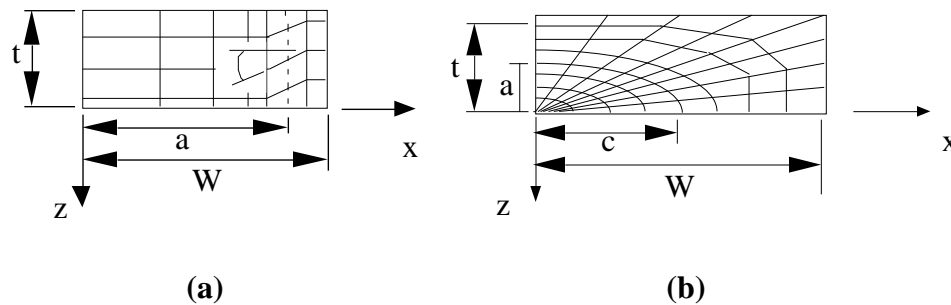


**Figure 5.** The crack plane of two general models:  
*a) rotated model, b) scaled model.*

## Finite-Element Analysis

The crack configurations that were studied were presented in Fig. 1. These solids are assumed to be of isotropic material with Poisson's ratio of 0.3. The solids are subjected to remote tensile loading to create only Mode I deformations at the crack front. Utilizing symmetry conditions one-eighth or one-quarter of each solid is modeled. The solids are modeled using eight-node hexahedral elements everywhere except at the crack tip where collapsed hexahedral or singularity elements are used. The finite-element models are developed using a modified version of the GENSURF program developed by Raju [10] and are analyzed using a modified version of the SURF3D program developed by Raju and Newman [11].

## RESULTS AND DISCUSSION

The stress-intensity factor values obtained from the through-the-thickness crack, the embedded elliptic crack, and the semi-elliptic surface crack are presented in this section. In each case the stress-intensity factor values obtained from the normal models are presented first and compared to the reference values for that configuration. Then, the stress-intensity factor values obtained from the general models using both the original formulations and the new formulations of the extraction methods are presented and compared to the values obtained from the orthogonal models.

### Through-the-Thickness Crack

The first crack configuration studied was a through-the-thickness crack in a large plate with  $(a/W) = 0.8$  and  $(a/h) = 0.01$  (See Fig. 1(a)). One-eighth of the solid was modeled using symmetric boundary conditions. The  $z$ -direction displacements of all of the nodes on the  $z = 0$  and  $z = t$  planes were prescribed zero to simulate the plane strain condition.

A three-dimensional orthogonal model was constructed with 10 equally spaced through-thickness layers. The model had 4378 nodes and 3580 elements. A typical finite-element mesh around the crack front perpendicular to the crack plane is shown in Fig. 6. This finite-element mesh was used for all of the models in this analysis and consisted of 10 rings and 8 radial wedges around the crack front. A general model was created by rotating the mesh near the crack front through a specified angle from the normal to the crack front. A  $30^\circ$  angle was chosen for the rotation at the nine interior stations on the crack front.

The stress-intensity factors were evaluated at the eleven nodes along the crack front. As expected, the value remained constant through the thickness. The normalized stress-intensity factor values obtained from the normal models using the standard formulations of the extraction methods are presented in Table 1. These values are compared to the reference value for this configuration given in Murakami *et al.* [10]. All of the stress-intensity factor extraction methods yielded stress-intensity factor values within 2% of the reference value for this configuration.

The stress-intensity factors for the general models were then evaluated using the COD, Force, VCCT, and EDI methods. In Figs. 7-10 the normalized stress-intensity factor values are plotted against the ratio of position through-the-thickness to total thickness ( $z/t$ ) for the orthogonal and general models.

The values obtained from the general model using the COD method, Force method and VCCT were 7% below the values extracted from the normal models. The EDI method remained unaffected by the lack of orthogonality at the crack front. The stress-intensity factor values of the general models were evaluated a second time using the new formulations that were developed for general models. The values obtained using the new formulations of the COD method, Force method and VCCT are plotted in Figs. 11-13. The stress-intensity factor values obtained from the orthogonal models are also plotted for comparison. Normalized stress-intensity factor values are plotted against the ratio of position through the thickness to total thickness ( $z/t$ ). The new formulations recovered the values obtained from the orthogonal models.

**Table 1.** Normalized stress-intensity factors for the through-the-thickness crack.

	$\frac{K_I}{S\sqrt{a}}$	Percent Error
Force	1.816	0.9
COD	1.802	0.2
VCCT	1.816	0.9
EDI	1.820	1.2
Ref. Val.[10]	1.799	-

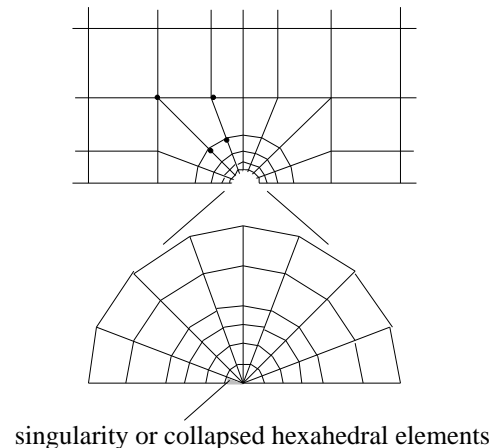


**Figure 6.** Finite-element crack tip mesh.

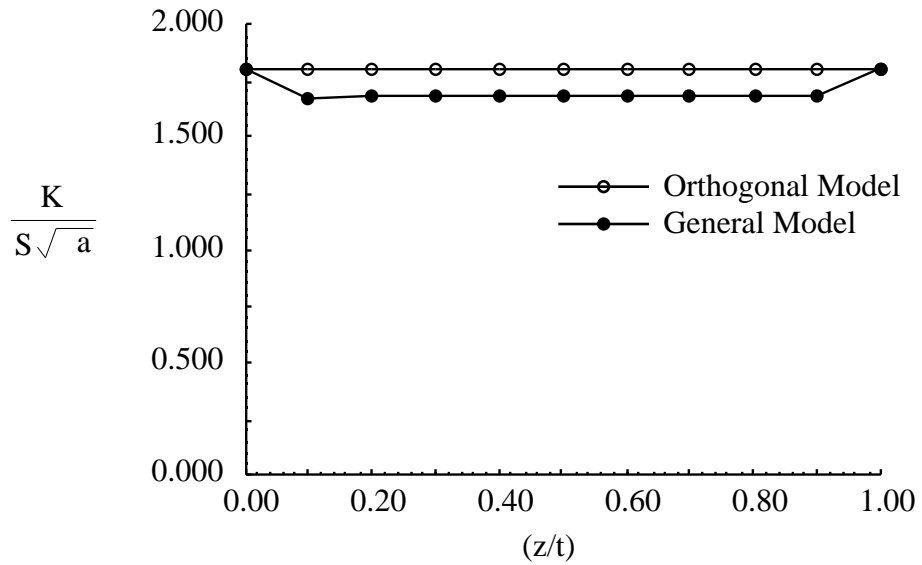


**Figure 7.** Stress-intensity factors evaluated for a through-the-thickness crack using the COD method.

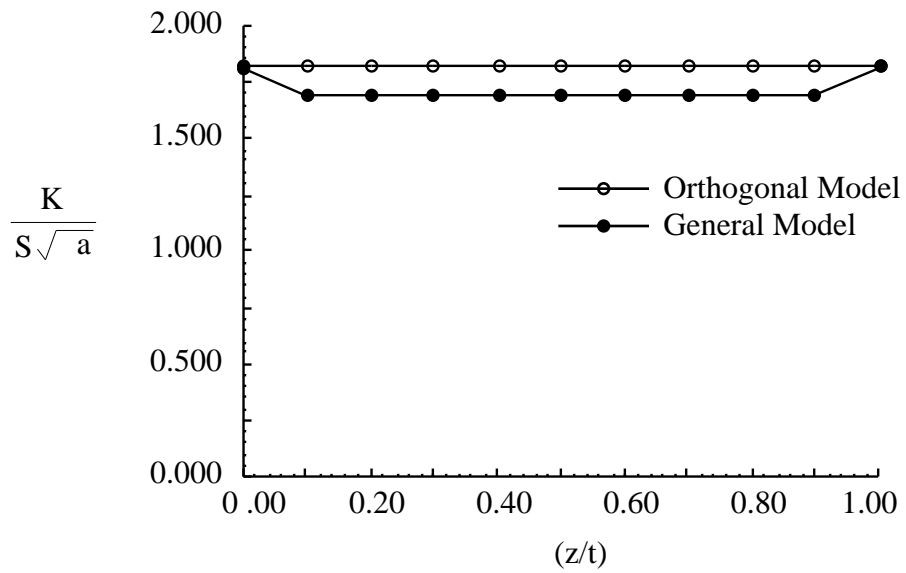


**Figure 8.** Stress-intensity factors evaluated for a through-the-thickness crack using the Force method.

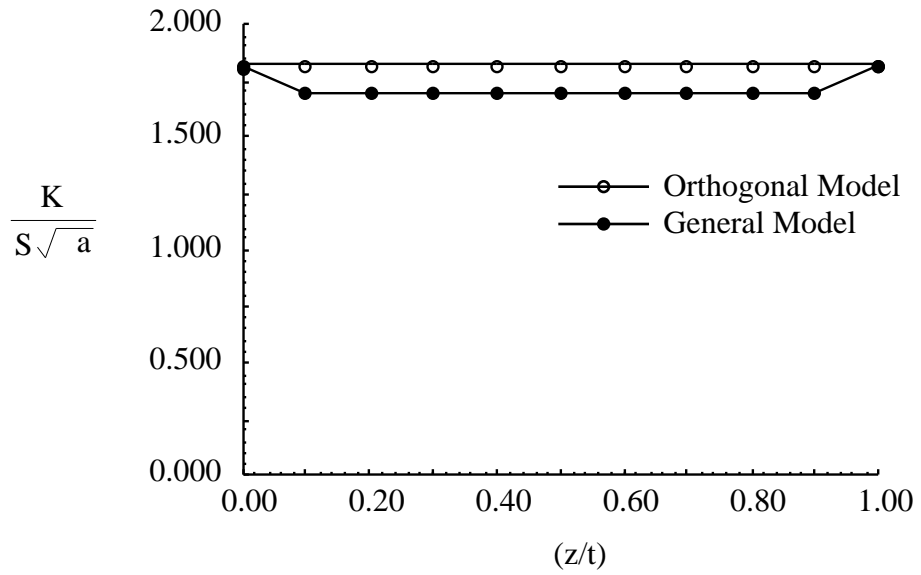


**Figure 9.** Stress-intensity factors evaluated for a through-the-thickness crack using the VCCT.

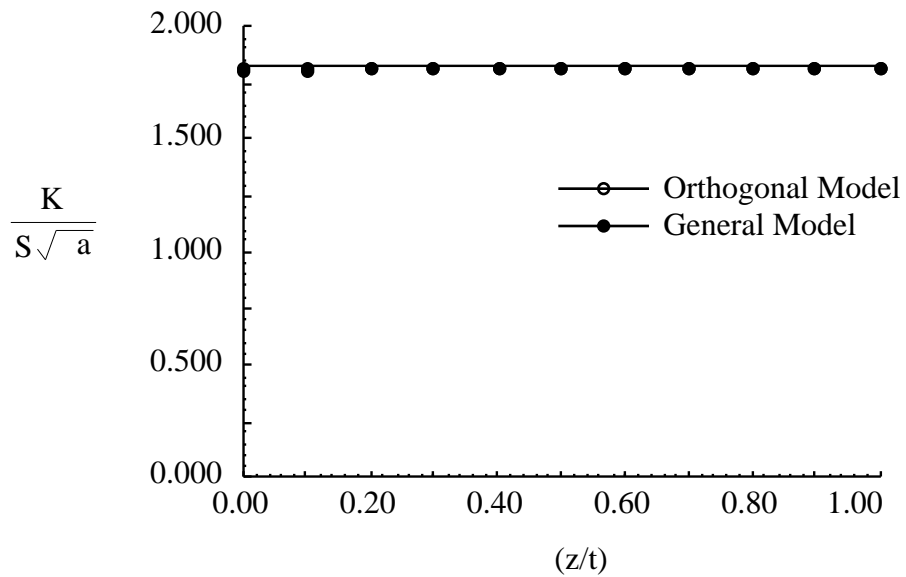


**Figure 10.** Stress-intensity factors evaluated for a through-the-thickness crack using the EDI method.

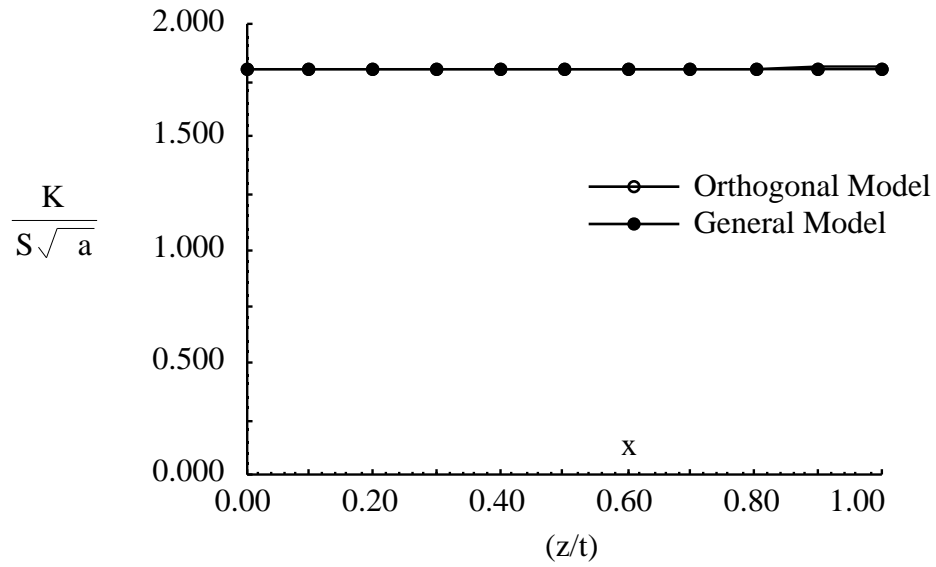


**Figure 11.** Stress-intensity factors evaluated for a through-the-thickness crack using the COD method formulated for general models.

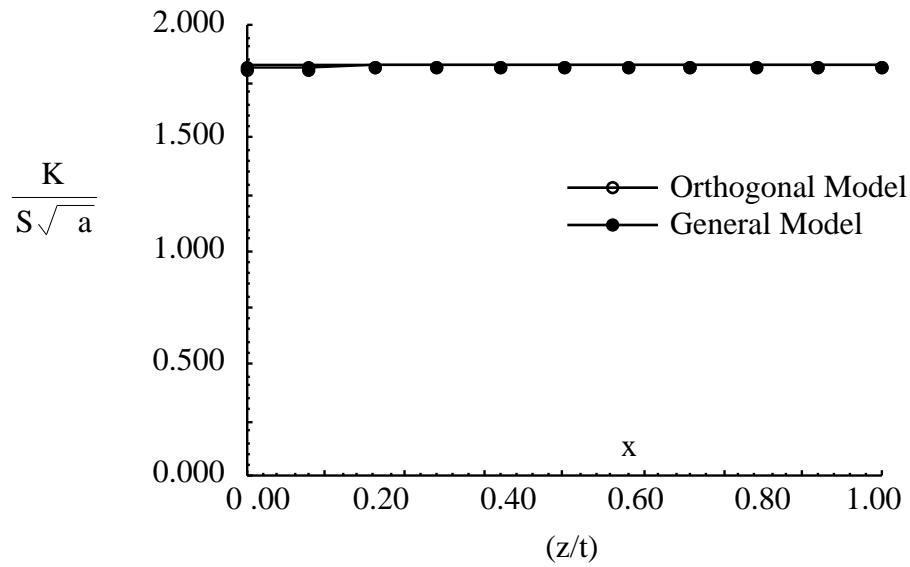


**Figure 12.** Stress-intensity factors evaluated for a through-the-thickness crack using the Force method formulated for general models.

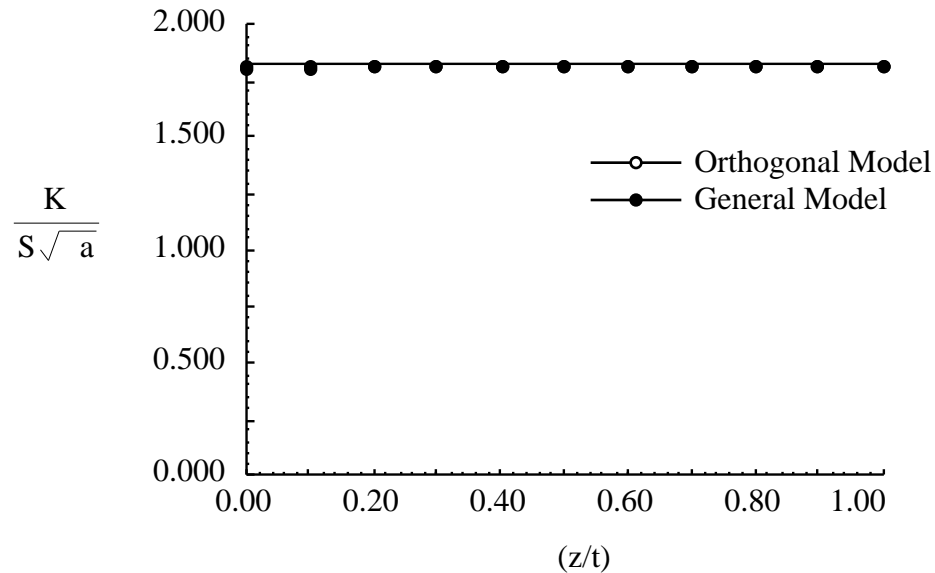


**Figure 13.** Stress-intensity factors evaluated for a through-the-thickness crack using the VCCT formulated for general models.

### Embedded Elliptic Crack

An embedded elliptic crack in a large solid,  $(a/t) = 0.2$ , with  $(a/h) = 0.01$ ,  $(h/w) = 0.5$ ,  $(a/c) = 0.2$  (see Fig. 1(b)) subjected to remote tensile loading was analyzed next. The crack front parameters  $a$ ,  $c$ , and  $\theta$  are shown in Fig. 14. One-eighth of the solid was modeled using symmetry boundary conditions. Two three-dimensional finite-element models were developed. Each model consisted of 4142 nodes and 3284 elements. The finite-element mesh around the crack front and perpendicular to the plane of the crack was the same as the mesh used for the through-the-thickness crack (see Fig. 6). Both models had nine stations on the crack front.

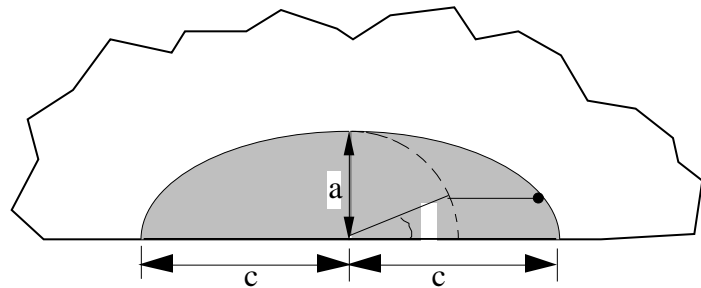


**Figure 14.** Crack front parameters for the elliptic crack configurations studied.

The orthogonal model was created using a conformal mapping to ensure orthogonality of the mesh at the crack front as described in Ref. [11]. The general model was created using a constant coordinate scaling which resulted in a model of the type shown in Fig 5(b). The mesh of the general model had varying degrees of rotation from the orthogonal condition. The angles that the crack tip mesh made with the crack front normals (average normals), presented in Table 2, demonstrate the severity of scaled mesh.

The stress-intensity factor values were evaluated at the nine nodes located on the crack front. The normalized stress-intensity factors obtained from the orthogonal model are shown in Table 3. These values are compared to the exact solution obtained by Green and Sneddon for an embedded elliptic crack in an infinite solid [13]. All of stress-intensity factor values except those at the first two stations on the crack front were within 2% of the analytical solution. Because of the extreme aspect ratio of the ellipse, the slope of the crack front is not accurately modeled at the first two stations on the crack front and the calculated stress-intensity factor values are not accurate in this region. Further mesh refinement in the region near  $\theta = 0$  is expected to increase the accuracy of the solution in this region.

The stress-intensity factors values of the general models were evaluated using the direct methods. The stress-intensity factor values obtained at each node on the crack front are plotted in Figs. 16-19. In these figures the normalized stress-intensity factor is plotted against the angular location along the crack front. The values obtained from the orthogonal models are also included in these figures for comparison.

The values obtained using the standard formulations of the extraction methods were up to 40% lower than the values obtained from the normal models. The EDI method remained unaffected by the lack of orthogonality at the crack front and yielded accurate values from the general meshes.

The stress-intensity factor values of the scaled model were re-evaluated using the formulations of the extraction methods developed for general models. These values are presented in Figs. 20-22. The new formulations were able to recover stress-intensity factor values within 3% of values that were obtained from the normal models. The COD method does not seem to recover as accurate stress-intensity factor values as the Force method and VCCT.

**Table 2.** Rotation of the crack tip mesh from the normal condition.

Parametric Angle ( $2 / \pi$ )	Rotation Angle
	a/c = 0.2
0.000	0.00
0.125	42.57
0.250	59.49
0.375	65.72
0.500	67.38
0.625	65.72
0.750	55.49
0.875	42.57
1.000	0.00

**Table 3.** Normalized stress-intensity factor values ( $K_I/S\sqrt{a/Q}$ ) for a shallow ( $a/t = 0.2$ ) embedded elliptic crack with ( $a/c$ ) = 0.2

Parametric Angle ( $2 / \pi$ )	Green and Sneddon [13]	COD	Force	VCCT	EDI
0.000	0.44721	0.42214	0.53072	0.47186	0.48373
0.125	0.52598	0.52052	0.56002	0.55001	0.55334
0.250	0.65189	0.65124	0.65169	0.66242	0.65983
0.375	0.76153	0.76736	0.75944	0.77101	0.76774
0.500	0.84918	0.85771	0.85074	0.85974	0.85809
0.625	0.91589	0.92398	0.92003	0.92659	0.92655
0.750	0.96283	0.96946	0.96851	0.97320	0.97417
0.875	0.99074	0.99608	0.99727	1.00070	1.00230
1.000	1.00000	1.00480	1.00680	1.00990	1.01150

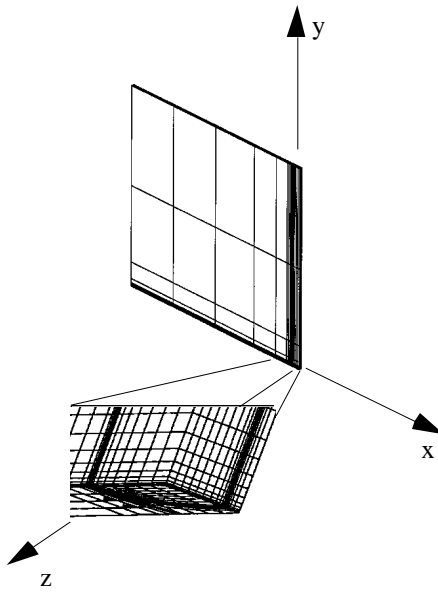


**Figure 15.** A typical finite-element model used to evaluate the stress-intensity factors of an elliptic crack .

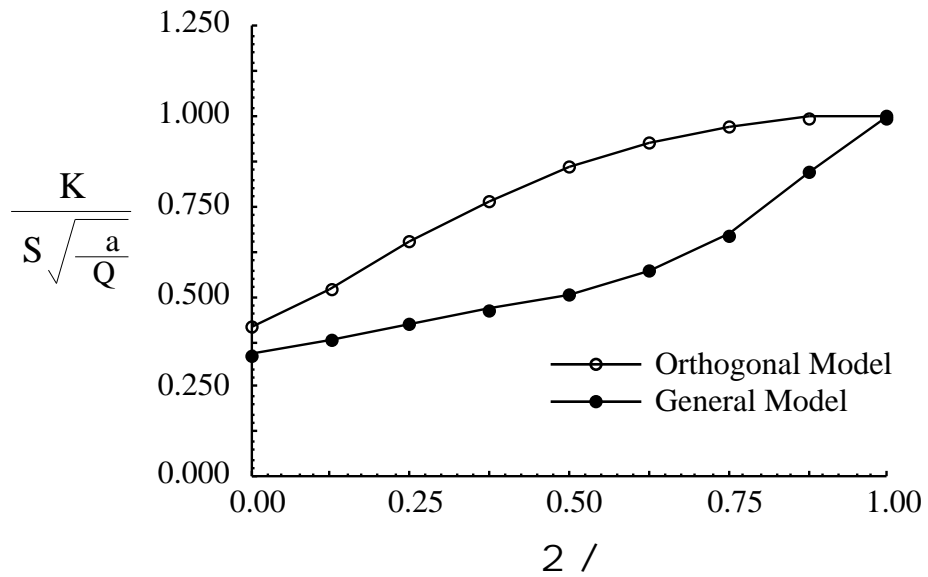


**Figure 16.** Stress-intensity factors evaluated for an embedded elliptic crack using the COD method.

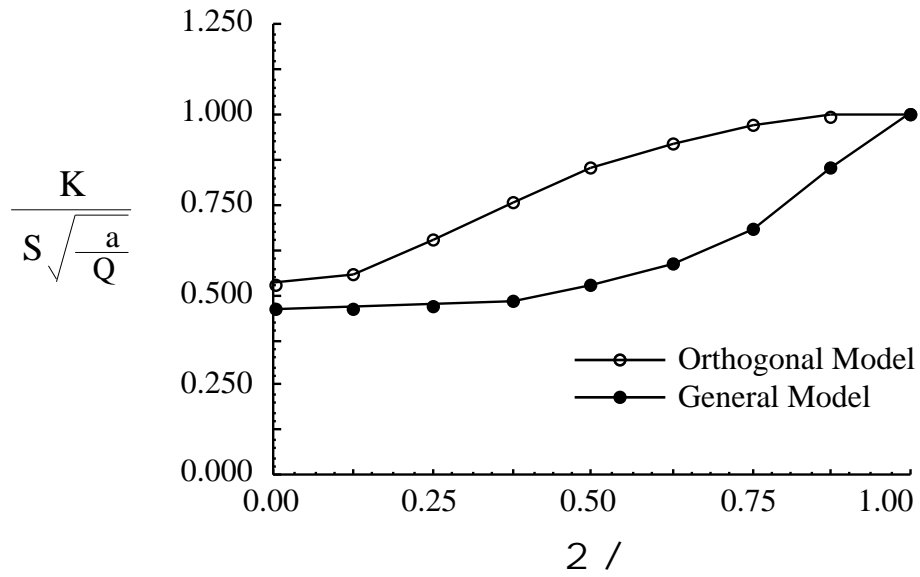


**Figure 17.** Stress-intensity factors evaluated for an embedded elliptic crack using the Force method.

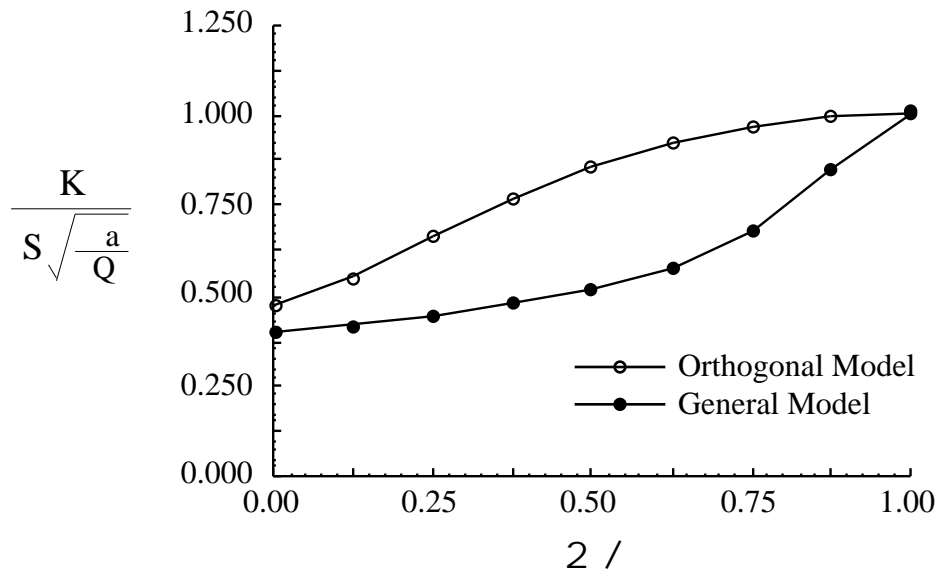


**Figure 18.** Stress-intensity factors evaluated for an embedded elliptic crack using the VCCT.

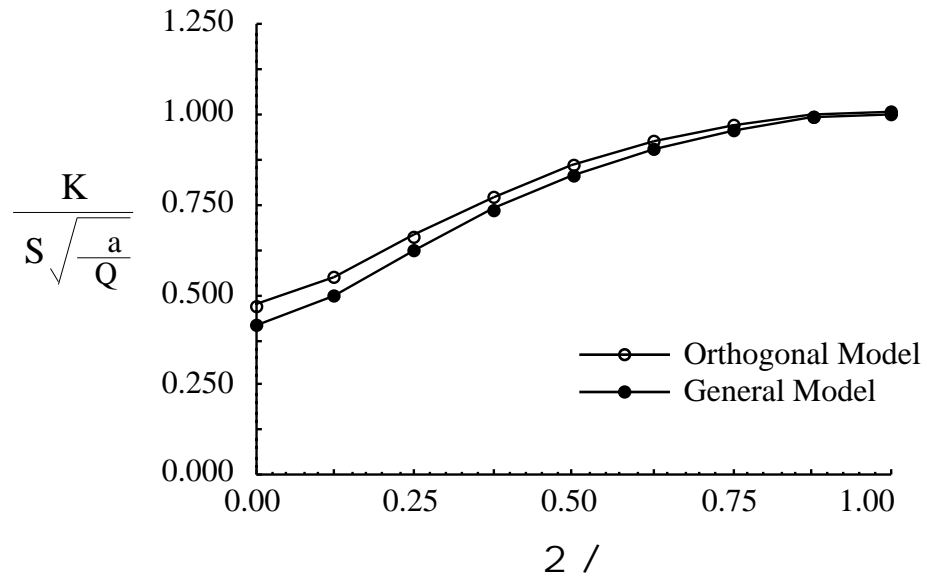


**Figure 19.** Stress-intensity factors evaluated for an embedded elliptic crack using the EDI method.

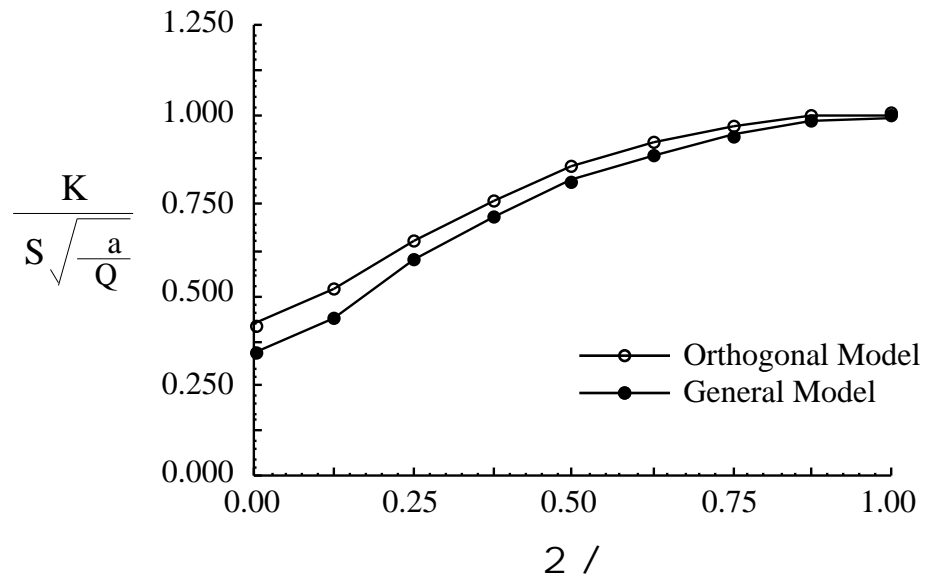


**Figure 20.** Stress-intensity factors evaluated for an embedded elliptic crack using the COD method formulated for general models.

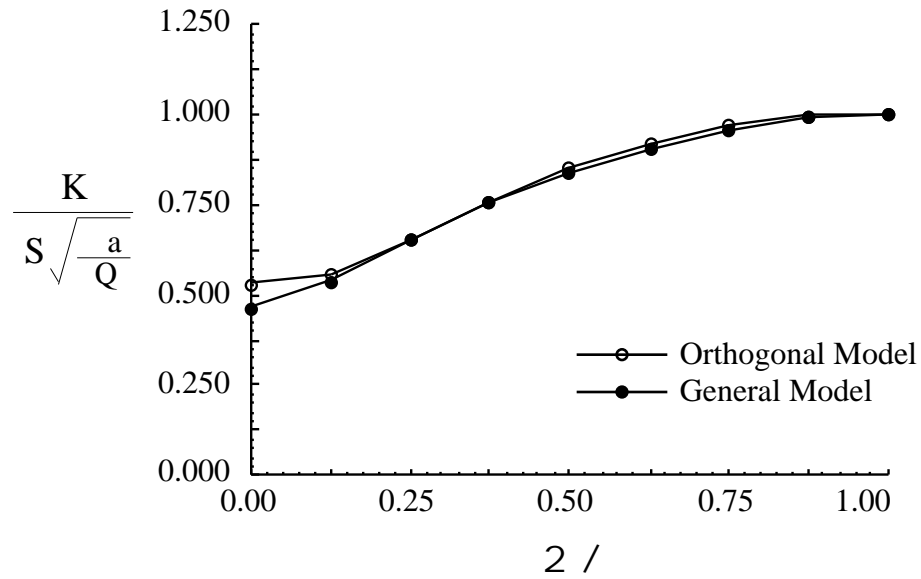


**Figure 21.** Stress-intensity factors evaluated for an embedded elliptic crack using the Force method formulated for general models.

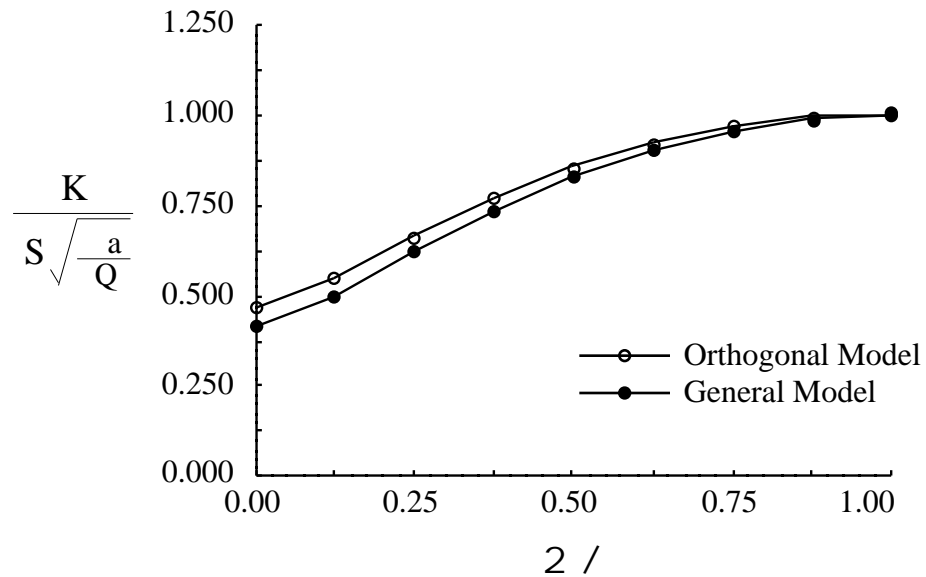


**Figure 22.** Stress-intensity factors evaluated for an embedded elliptic crack using the VCCT method formulated for general models.

### Semi-Elliptic Surface Crack

The third configuration studied was a deep semi-elliptic surface crack ( $a/c = 0.2$ ,  $a/t = 0.8$ ) in a large plate ( $a/W = a/h = 0.01$ ) subjected to remote tensile loading. Using symmetric boundary conditions, one-quarter of the solid was modeled. Two three-dimensional models, orthogonal and general (scaled), were created in the same manner as discussed for the embedded elliptic crack configuration. Each model consisted of 4142 nodes and 3284 elements.

The stress-intensity factors of the orthogonal models were evaluated using the Force, COD, VCCT, and EDI methods. The stress-intensity factor was evaluated at the nine nodes located on the crack front. The normalized stress-intensity factors obtained from the normal model are presented in Table 4. These values are compared to the numerical solution obtained by Raju and Newman [12]. The stress-intensity factor extraction methods obtained stress-intensity factor values within 5% of the reference values for all but the first two stations along the crack front. Because of the rapid transition from plane strain to plane stress at the free surface ( $\theta = 0$ ) and the difficulty associated with modeling the crack front, accurate values could not be obtained at these two stations. Further mesh refinement in this region would increase the accuracy of the solution.

The stress-intensity factors of general models were then evaluated using the stress-intensity factor extraction methods. The stress-intensity factor values obtained at each node on the crack front are presented in Figs. 23-26. In these figures the normalized stress-intensity factors are plotted against the parametric angle (location on the crack front) for both orthogonal and general models. The stress-intensity factor values obtained from the general models were as much as 40% lower than the values obtained from the orthogonal models. The EDI method remained unaffected by the lack of orthogonality at the crack front and yielded accurate stress-intensity factors.

**Table 4.** Normalized stress-intensity factor values ( $K_I/S\sqrt{a/Q}$ ) for a deep ( $a/t = 0.8$ ) semi-elliptic surface crack with ( $a/c = 0.2$ )

Parametric Angle ( $2\theta$ )	Ref. Val. [12]	COD	Force	VCCT	EDI
0.000	1.1510	0.9531	1.1065	1.0264	1.0190
0.125	1.1526	0.9772	1.0674	1.0396	1.0568
0.250	1.2732	1.1815	1.1788	1.2000	1.1990
0.375	1.4208	1.3585	1.3421	1.3641	1.3620
0.500	1.5629	1.4946	1.4828	1.4988	1.5003
0.625	1.6680	1.6053	1.5934	1.6076	1.6082
0.750	1.7388	1.6610	1.6576	1.6666	1.6699
0.875	1.7657	1.6832	1.6864	1.6918	1.6970
1.000	1.7718	1.6885	1.6941	1.6982	1.7042

The stress-intensity factor values for the general model were re-evaluated using the formulations of the extraction methods developed for general models. These values are plotted in Figs. 27-29. The new formulations were able to recover stress-intensity factor values within 3% of values that were obtained from the orthogonal models.

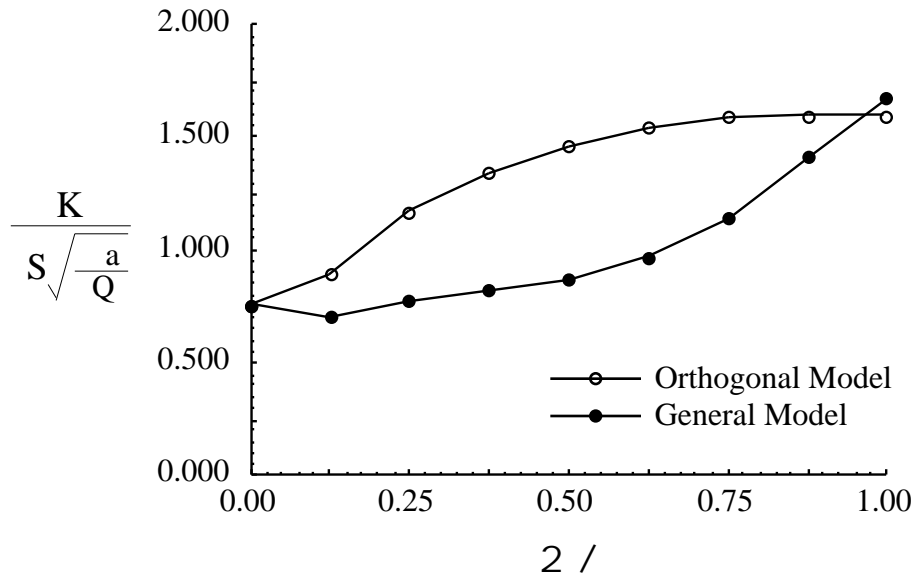


**Figure 23.** Stress-intensity factors evaluated for a semi-elliptic surface crack using the COD method.

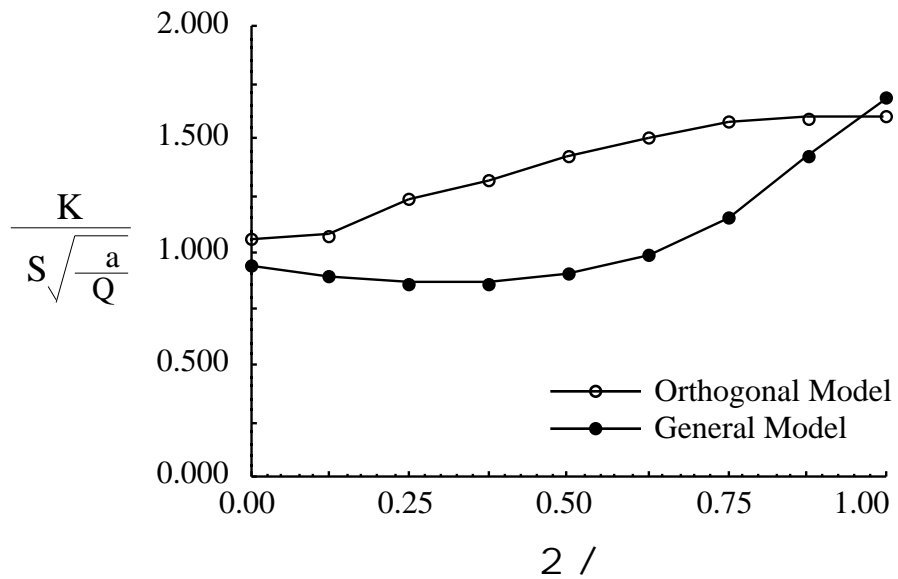


**Figure 24.** Stress-intensity factors evaluated for a semi-elliptic surface crack using the Force method.

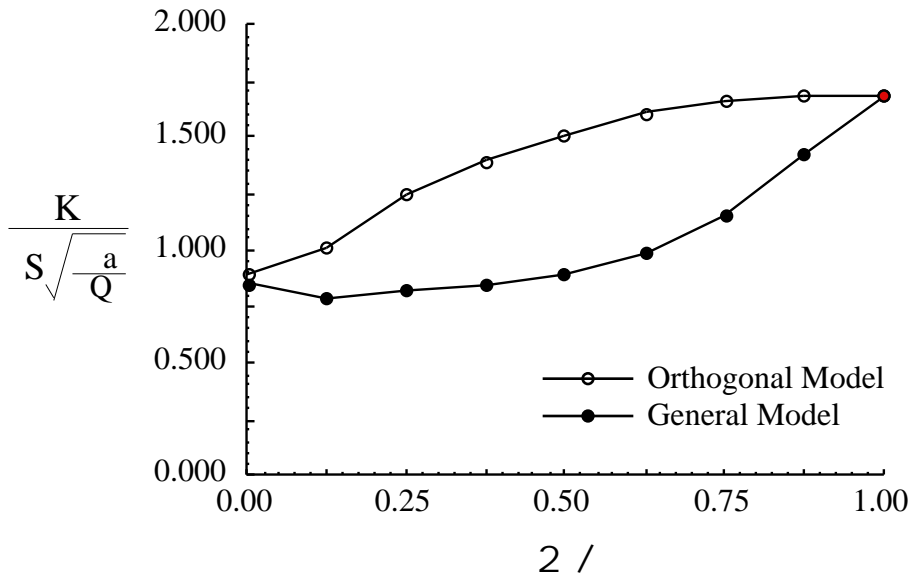


**Figure 25.** Stress-intensity factors evaluated for a semi-elliptic surface crack using the VCCT.

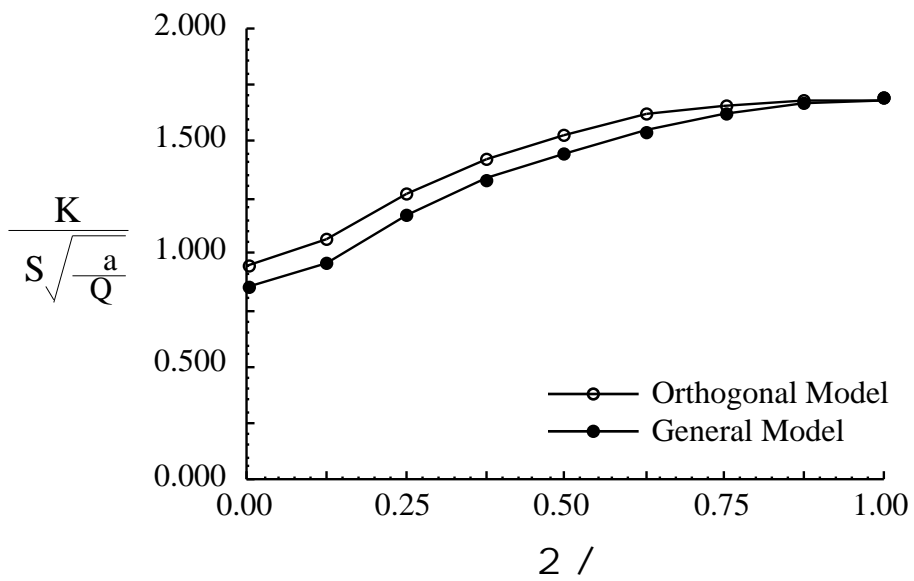


**Figure 26.** Stress-intensity factors evaluated for a semi-elliptic surface crack using the EDI method.

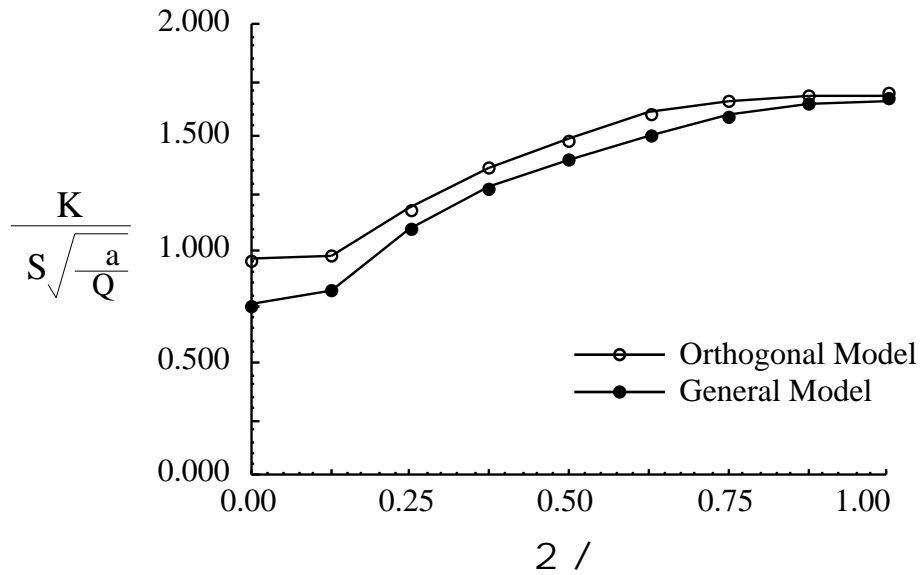


**Figure 27.** Stress-intensity factors evaluated for a semi-elliptic surface crack using the COD method formulated for general models.

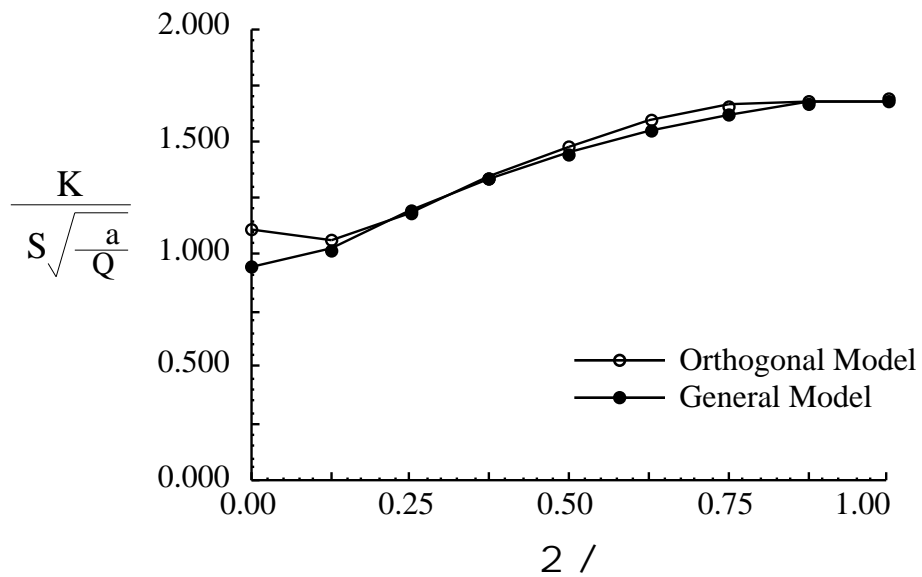


**Figure 28.** Stress-intensity factors evaluated for a semi-elliptic surface crack using the Force method formulated for general models.

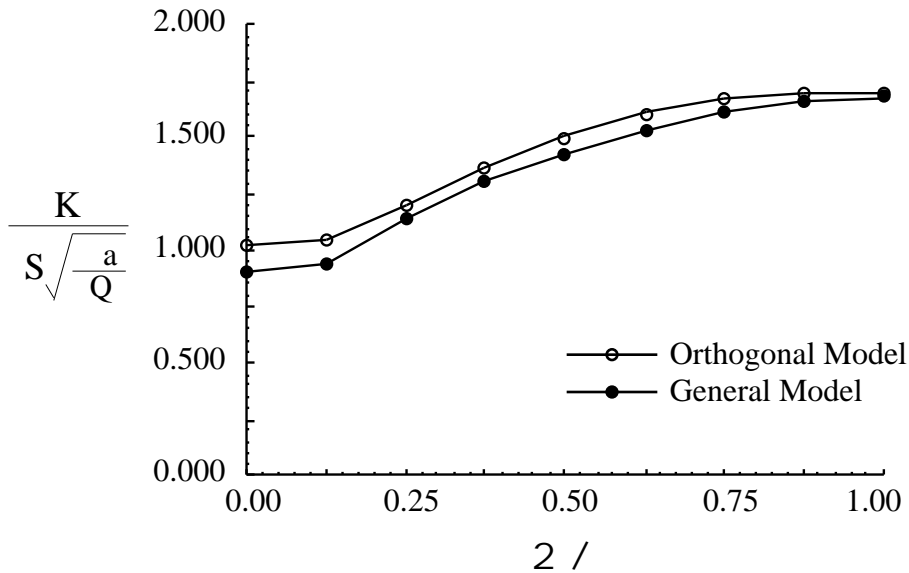


**Figure 29.** *Stress-intensity factors evaluated for a semi-elliptic surface crack using the VCCT formulated for general models.*

## Concluding Remarks

Finite-element models with and without mesh orthogonality at the crack front were developed for a through-the-thickness crack, an embedded elliptic crack, and a semi-elliptic surface crack. These models were subjected to remote tensile loads to generate Mode I displacements at the crack front. Stress-intensity factors were calculated for these models using the Crack-Opening-Displacement (COD) method, Force method, Virtual-Crack-Closure technique (VCCT), and the Equivalent Domain Integral (EDI) method. The direct methods (COD method, Force method and VCCT) were unable to obtain accurate stress-intensity factors from the models without orthogonality at the crack front. The EDI obtained accurate stress-intensity factors from models with and without orthogonality at the crack front.

Careful consideration of the formulations of the direct methods and the definitions of stress-intensity factor and strain-energy release rate reveal an implicit assumption that an orthogonal mesh is present at the crack front. Due to this assumption these methods cannot obtain accurate stress-intensity factor values unless re-formulated for general finite-element modeling. The development of the EDI method was based on an integral quantity that has no dependence on the form of the finite-element modeling near the crack tip. Hence, the EDI method remained unaffected by any lack of orthogonality near the crack front.

New formulations of the COD method, Force method, and VCCT, were developed to evaluate stress-intensity factors for general models that lack orthogonality at the crack front. These new formulations use the values of force and displacement at the nodes in front of and behind the crack tip which do not lie on the normal to the crack front. The force and opening nodes (the nodes in front of and behind the crack front, respectively) are used to project points onto the normals to the crack front. The radial distance, average element thickness, and crack-front extension area are calculated using the points projected

onto the normals to the crack front. Accurate stress-intensity factor values were obtained from general models using the new formulations of the extraction methods.

The new formulations developed in this paper were unable to extract accurate stress-intensity factor values in regions where the stresses changed rapidly along the crack front. This generally occurred in regions where the crack front met free surfaces or the shape of the crack front changed rapidly. The accuracy of the solutions obtained in these regions might be improved by local mesh refinement.

## References

- [1] Broek, David, *Elementary Fracture Mechanics*, 3d ed., Martinus Nijhoff Publishers, Boston, 1983.
- [2] Raju, I.S. and Newman, J.C. Jr., "Three-Dimensional Finite-Element Analysis of Finite-Thickness Fracture Specimens," *NASA TN D-8414*, National Aeronautics and Space Administration, Washington, DC, 1977.
- [3] Raju, I.S. and Newman, J.C. Jr., "Improved Stress-Intensity Factors for Semi-elliptic Surface Cracks in Finite-Thickness Plates," *NASA TM X-72825*, National Aeronautics and Space Administration, Washington, DC, 1977.
- [4] Rybicki, E.F. and Kanninen, M.F., "A Finite-Element Calculation of Stress-Intensity Factors by a Modified Crack Closure Integral," *Engineering Fracture Mechanics*, Vol. 9, 1977, pp. 931-938.
- [5] Shivakumar, K.N., Tan, P.W., and Newman, J.C., Jr., "A Virtual Crack Closure Technique for Calculating Stress-Intensity Factors for Cracked Three-Dimensional Bodies," *International Journal of Fracture*, Vol. 36, 1988, pp. R43-R50.
- [6] Nikishkov, G.P., and Atluri, S.N., "Calculation of Fracture Mechanics Parameters for an Arbitrary Three-Dimensional Crack, by the 'Equivalent Domain Integral'," *International Journal of Numerical Methods in Engineering*, Vol. 24, 1987, pp. 1801-1821.
- [7] Nikishkov, G.P., and Atluri, S.N., "An Equivalent Domain Integral Method for Computing Crack-Tip Parameters in Non-Elastic, Thermo-Mechanical Failure," *Engineering Fracture Mechanics*, Vol. 26, 1987, pp. 851-867.
- [8] Raju, I.S. and Shivakumar, K.N., "An Equivalent Domain Integral Method in the Two-Dimensional Analysis of Mixed Mode Crack Problems," *Engineering Fracture Mechanics*, Vol. 37, 1988, pp. 707-725.
- [9] Shivakumar, K.N. and Raju, I.S., "An Equivalent Domain Integral Method for Three-Dimensional Mixed Mode Fracture Problems," *Engineering Fracture Mechanics*, Vol. 42, 1992, pp. 935-959.
- [10] Murakami, Y., *et al.* (Eds), *Stress-Intensity Factors Handbook*, Vol. 1, Pergamon Press, Tokyo, 1987
- [11] Raju, I.S., "GENSURF: A mesh generator for 3D finite-element analysis of surface and corner cracks in finite thickness plates subjected to mode-I loadings," *NASA CR-189559*, 1992.

- [12] Raju, I.S. and Newman, J.C. Jr., "SURF3D: A 3D Finite-Element Program for the Analysis of Surface and Corner Cracks in Solids Subjected to Mode-I Loadings," *NASA TM-107710*, National Aeronautics and Space Administration, Washington, DC, 1993.
- [13] Green, A.E. and Sneddon, I.N., "The Distribution of Stress in the Neighborhood of a Flat Elliptic Crack in an Elastic Solid," *Proceedings of the Cambridge Philosophical Society*, Vol. 46, 1950, pp. 159-164.